Chemical Science

Accepted Manuscript

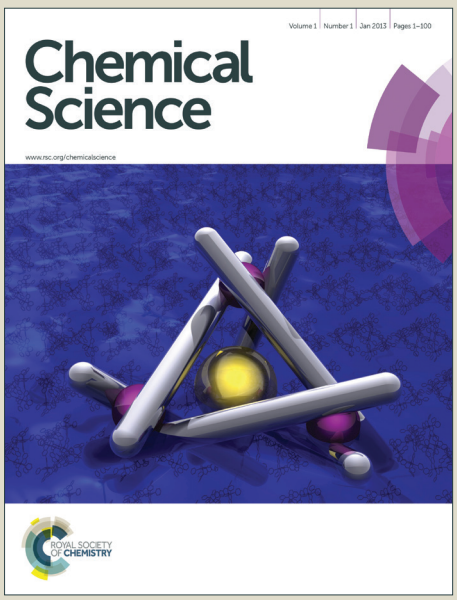

This is an *Accepted Manuscript*, which has been through the Royal Society of Chemistry peer review process and has been accepted for publication.

Accepted Manuscripts are published online shortly after acceptance, before technical editing, formatting and proof reading. Using this free service, authors can make their results available to the community, in citable form, before we publish the edited article. We will replace this *Accepted Manuscript* with the edited and formatted *Advance Article* as soon as it is available.

You can find more information about *Accepted Manuscripts* in the Information for Authors.

Please note that technical editing may introduce minor changes to the text and/or graphics, which may alter content. The journal's standard Terms & Conditions and the Ethical guidelines still apply. In no event shall the Royal Society of Chemistry be held responsible for any errors or omissions in this *Accepted Manuscript* or any consequences arising from the use of any information it contains.

ROYAL SOCIETY OF CHEMISTRY

www.rsc.org/chemicalscience

Chemical Science

RSCPublishing

ARTICLE

Mechanistic Studies on Covalent Assemblies of Metal-Mediated Hemi-Aminal Ethers†

Cite this: DOI: 10.1039/xoxxoooooox

Hyun Hwa Jo,[a] Ramakrishna Edupuganti, [a,c] Lei You, [b] Kevin N. Dalby [c] and Eric V. Anslyn* [a]

Received ooth ZZZ 2014,
Accepted ooth ZZZ 2014

DOI: 10.1039/xoxxoooooox

www.rsc.org/

The use of reversible covalent-bonding in a four-component assembly incorporating chiral alcohols was recently reported to give a method for determining the enantiomeric excess of the alcohols via CD spectroscopy. Experiments that probe the mechanism of this assembly, which consists of 2-formylpyridine (**2-PA**), dipicolylamine (**DPA**), Zn(II), and alcohols, to yield zinc-complexes of tren-like ligands, are presented. The studies focus upon the mechanism of conversion of a hemi-aminal (**1**) to a hemi-aminal ether (**3**), thereby incorporating the fourth component. It was found that molecular sieves along with 3 to 4 equivalents of alcohol are required to drive the conversion of **1** to **3**. Attempts to isolate an intermediate in this reaction via addition of strong Lewis-acids led to the discovery of a five-membered ring pyridinium salt (**5**), but upon exposure to Zn(II) and alcohols gave different products than the assembly. This was interpreted to support the intermediacy of an iminium species. Kinetic studies reveal that the conversion of **1** to **3** is zero-order in alcohol in large excesses of alcohol, supporting rate-determining formation of an intermediate prior to reaction with alcohol. Further, the magnitude of the rate constant for interconversion of **1** and **3** are similar, supporting the notion that there are similar rate-determining steps (rds's) for the forward and reverse reactions. Hammett plots show that the rds involves creation of a negative charge (interpreted as the loss of positive charge), supporting the notion that decomplexation of Zn(II) from the assemblies to generate apo-forms of **1** and **3** is rate-determining. The individual mechanistic conclusions are combined to create a qualitative reaction coordinate diagram for the interconversion of **1** and **3**.

Introduction

Dynamic Covalent Bonding (DCB) can be used to exchange molecular components to reach the thermodynamic minima of a system.[1-6] In recent decades, DCB has been explored due to applicability in supramolecular chemistry.[7-10] For example, DCB is useful to create new molecular receptors, protein ligands, and sensors.[11-15] It is quite common to combine metal-coordination or donor-acceptor interactions with dynamic covalent bonds. [13,16]

One application to which DCB has been applied is the determination of chirality. The discrimination of chiral compounds is essential in the pharmaceutical industry where enantiomeric purity of chiral drugs can greatly influence therapeutic and biological properties.[17] Much effort has been devoted to creating methods that report the enantiomeric excess (*ee*) of target chiral building blocks using supramolecular and dynamic covalent bond chemistry.[18-20]

Our group reported a one-pot protocol involving multiple dynamic covalent bonds which target chiral alcohols.[21] This system forms a hemi-aminal (**1**) from three components which subsequently forms a hemi-aminal ether (**3**) from a fourth component (alcohol) upon dehydration (**Scheme 1**). The reversibility of the covalent bonds in this assembly enables the exchange of all four components.[22] The use of the assembly to measure *ee* values of alcohols has been covered in depth.[21,23,24] In this paper, a mechanistic investigation of this multi-component assembly is reported. Understanding the mechanism

[a] *Department of Chemistry, The University of Texas at Austin, Austin, Texas, 78712, USA. E-mail: anslyn@austin.utexas.edu*

[b] *Fujian Institute of Research on the Structure of Matter, Chinese Academy of Sciences, Fuzhou, 350002, P.R.China. E-mail: lyou@fjirsm.ac.cn*

[c] *Division of Medicinal Chemistry, The University of Texas at Austin, Austin, Texas, 78712, USA. E-mail: dalby@austin.utexas.edu*

† Electronic Supplementary Information (ESI) available: See DOI: 10.1039/b000000x/

Chemical Science Accepted Manuscript

of this assembly should enable further exploitation of dynamic hemi-aminal ether formation in a variety of contexts.[25-27]

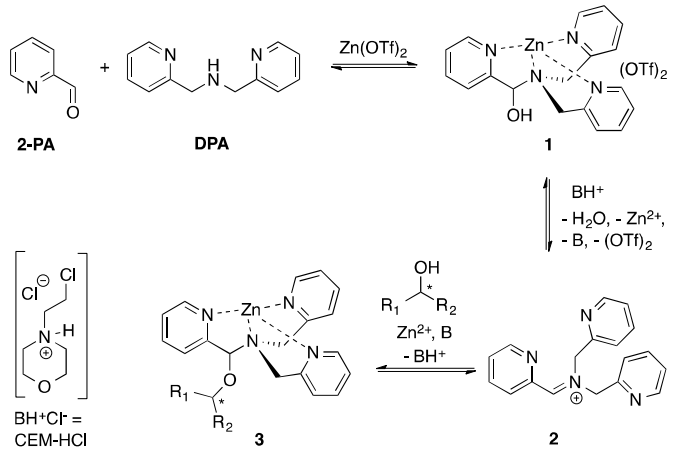

Scheme 1. Reversible multicomponent-assembly for the binding of chiral secondary alcohols.

Results and Discussion

I. Extent of Alcohol Incorporation in Multi Component Assembly

In our previous papers describing the use of the four-component assembly given in Scheme 1, we postulated that the reaction proceeded via iminium ion **2**, which would then add alcohols to create hemi-aminal ethers that are thermodynamically stabilized via binding of Zn(II) to the tren-like ligand.[21] Molecular sieves play a major role in the assembly process by scavenging water to drive the equilibrium involving alcohol incorporation. Depending on the absence or presence of molecular sieves in solution, the alcohol incorporation jumps from 40% to 90%, respectively (**Table 1**). Further, the Brønsted acid (CEM-HCl), used as a catalyst, is critical to the assembly. Without a Brønsted acid, no hemi-aminal ether is formed (**Table 1**). It was found that CEM-HCl is the most effective acid catalyst, and led to the best yield of the hemi-aminal ether complex when Brønsted acids were screened.[21] CEM-HCl forms 3,12-dioxa-6,9-diazoniadispiro[5.2.5.2]hexadecane in the presence of **DPA** by slowly releasing hydrochloric acid (**Scheme 2**).[28]

# of sieves	Brønsted acid	% Alcohol incorporation
0	N	0
0	Y	40
2	N	0
2	Y	88
4	N	0
4	Y	90

Table 1. Percent yield of hemi-aminal ether complex when number of molecular sieves (3Å) and presence of Brønsted acid were varied. (Concentration of **2-PA**: 35 mM, **DPA**: 42 mM, alcohol: 175 mM and Zn(II) : 35 mM in acetonitrile).

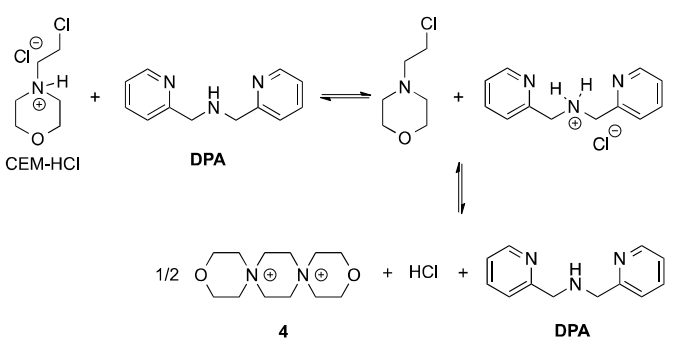

Scheme 2. Pathway of CEM-HCl to form 3,12-dioxa-6,9-diazoniadispiro[5.2.5.2]hexadecane releasing HCl.

In addition to the necessity of molecular sieves, one needs an excess of alcohol to drive the assembly to completion. Figure 1A shows the yield of the assembly as a function of the number of equivalents of an alcohol (4-penten-2-ol). As previously reported, the assembly with chiral alcohols results in circular dichroism (CD) signals. Figure 1B displays the CD intensity as a function of alcohol concentration, which shows that an excess of the alcohol is required to ensure complete assembly. To ensure saturation in the assembly reactions, all experiments for *ee* determination are conducted using 3 equiv. or more of alcohol.

Because molecular sieves and excess alcohol is required to drive the reaction to completion, it was anticipated that the value of the equilibrium constant (K_{eq}) between **1** and **3** must be less than 1. The ^{1}H-NMR chemical shifts of **1** and **3** are distinct, and thus it is a simple matter of integration of the respective resonances to measure a K_{eq} value, along with knowledge of the starting concentrations of all reactants: **1** and alcohol, and a controlled amount of water (Eq. 1). Thus, with an initial concentration of **1** being 35 mM, water at 35 mM, and alcohol at 175 mM, Eq. 1 yielded a K_{eq} value of 0.042.

$$K_{eq} = \frac{[\mathbf{3}][H_2O]}{[\mathbf{1}][ROH]} \qquad \text{(Eq. 1)}$$

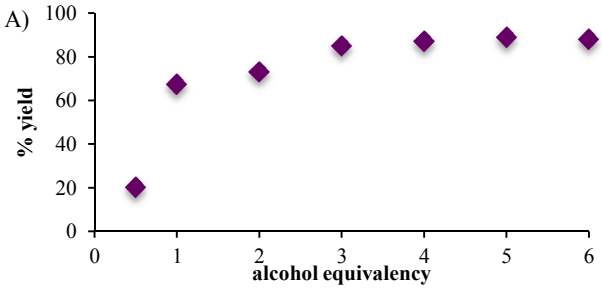

Chemical Science Accepted Manuscript

This journal is © The Royal Society of Chemistry 2014

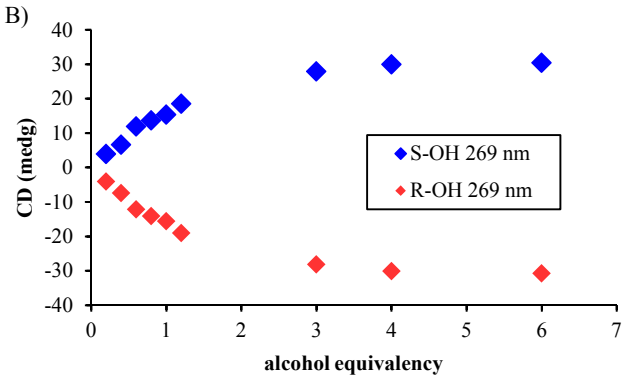

Figure 1. A) The percent yields and B) CD intensities of hemi-aminal ether formation when the equivalency of alcohol was varied. (Concentration of **2-PA**: 35 mM, **DPA**: 42 mM and Zn(II) : 35 mM in acetonitrile).

II. Isolation and Characterization of the Intermediate

Although not commonly isolated, iminium salts have been characterized previously.[29] With this precedent in mind, we set out to create iminium **2** as a means to test its validity as the intermediate in the assembly process shown in Scheme 1. To isolate salt **2**, we used powerful Lewis acids such as TMS-OTf and BF_3-OEt_2 to facilitate **DPA** addition to **2-PA** (**Scheme 3**).

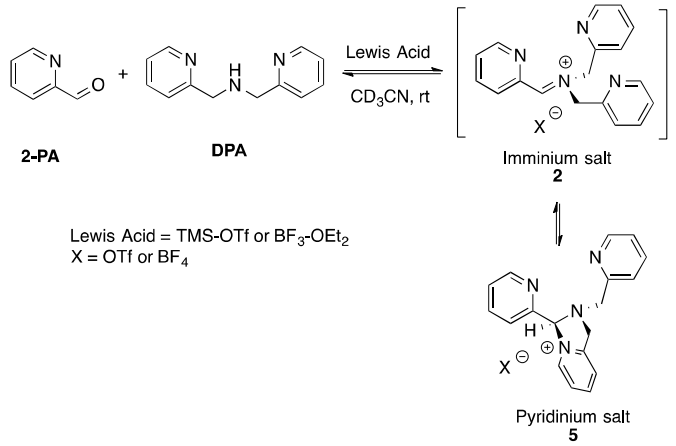

Scheme 3. Lewis acid assisted condensation and formation of a pyridinium salt. The cyclization of **2** to **5** is *5-endo-trig*, and thus not strictly allowed by Baldwin's rules.

In an NMR tube, upon addition of one equivalent of TMS-OTf or BF_3-OEt_2 to a mixture of **2-PA** and **DPA** in CD_3CN (60 mM), resonances for a new product along with unreacted **2-PA** were observed. The ^{1}H NMR spectrum was not consistent with **2** as the product because two inequivalent CH_2-groups were formed and the hydrogens on each CH_2 were diastereotopic (see supporting information). When excess BF_3-OEt_2 (more than 2 equiv.) was used to push the addition of **DPA** to completion in acetonitrile, a yellow precipitate was isolated at 0 °C. The precipitate was separated and crystals were grown by slow diffusion of diethyl ether into a solution of the yellow solid in acetonitrile at 0 °C. X-ray diffraction analysis revealed pyridinium salt **5**.

However, addition of water or alcohol and $Zn(OTf)_2$ to the pyridium salt **5** did not produce good yields of the hemi-aminal **1** or hemi-aminal ether **3,** respectively. Instead, a myriad of additional un-isolable products were created. Therefore, although while pyridinium salt **5** can be isolated, it must not actually be the correct intermediate formed in the assembly. We interpret this evidence as supporting iminium **2** as the true intermediate that reacts with water or an alcohol to create **1** or **3**, respectively. One rationalization for these results come from Baldwin's rules.[30,31] The cyclization of **2** to **5** is *5-endo-trig*, which is forbidden by these rules. A second rationalization comes from the expected lifetime of an iminum in the presence of water. For example, in water as the solvent, iminium ions have lifetimes on the order of only picoseconds.[32-35] Hence, irrespective of the intramolecularity of the pyridine, only in the absence of an external water or alcohol nucleophile does the cyclization occur. Apparently, in the presence of these nucleophiles their intermolecular addition outcompetes the intramolecular addition of pyridine.

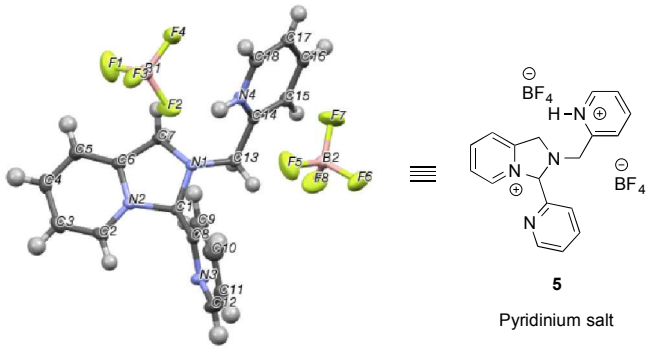

Figure 2. X-ray structure of pyridinium salt **5** created from 2-picolinaldehyde, dipicolylamine and excess BF_3-OEt_2.

III. Kinetics

As described above, the three-component assembly readily forms the hemi-aminal complex **1**, and with assistance of a Brønsted acid catalyst will create the hemi-aminal ether **3** in the presence of an alcohol. Therefore, to explore the mechanism of formation of **3** it was most convenient to start with preformed **1**. A plausible mechanism for the creation of **3** is given in Scheme 4. It starts with loss of Zn(II) from the tren-like ligand, followed by acid catalyzed elimination of water to create **2**. Given that **2** is the highest energy species along the sequence, either of the two steps prior to formation of **2** could be rate-determining. Thus, we set out to determine if loss of metal or elimination of water is the slow step leading to **2**.

Chemical Science Accepted Manuscript

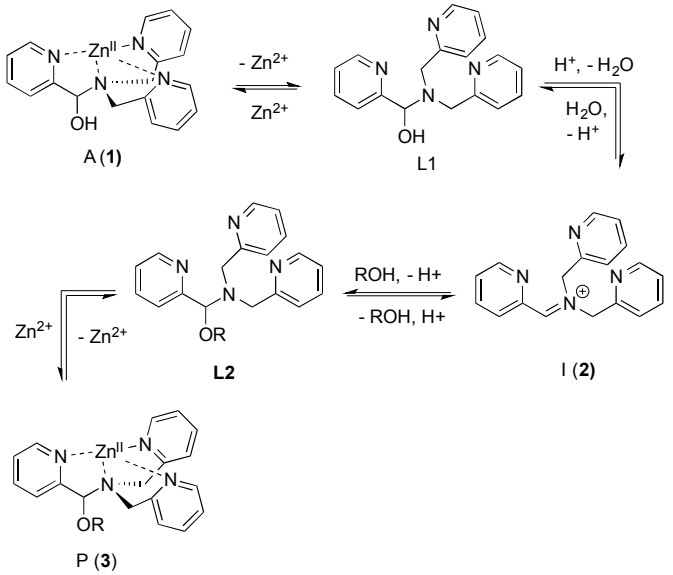

Scheme 4. Proposed pathway for interconverion of **1** and **3**.

As shown in Scheme 5, the two steps leading to the intermediate can be combined to simplify the mathematical analysis, although either of the two steps could be rate limiting. The form of the rate expression predicts a second order reaction at low concentrations of alcohol (first order in **1** and alcohol). To test this dependence, we analyzed the reaction as first order in **1** and zero-order in alcohol using three equivalents of alcohol (and no molecular sieves). The standard plot of ($\ln\{[A]_o / ([A]_o - [P])\}$) versus time gave a plot with significant curvature (**Figure 3**), therefore not conforming to first order kinetics. However, the rate expression predicts that the reaction should become increasing first order in **1** and zero-order in alcohol as the alcohol concentration increases. The mechanism is analogous to an S_N1 reaction where at high concentrations of nucleophile a zero order dependence of nucleophile is the norm. As seen in Figure 3, the kinetic plot becomes increasingly linear, and at 18 or more equivalents of alcohol the plot conforms nicely to pseudo-first order kinetics. Under these conditions the concentration of alcohol is large enough to compete with any residual water or water released during the reaction. The rate constant k_{-1} is predicted to be larger than k_2 due to a larger nucleophilicity of water relative to alcohols due to water's smaller size.[36] Thus, it takes an excess of alcohol to cause the rate expression to simplify to first order in **1** only. When 2 equivalents of water were added at this high concentration of alcohol, the rate drops drastically and the reaction loses first order behaviour, analogous to the common ion effect in an S_N1 reaction.[37]

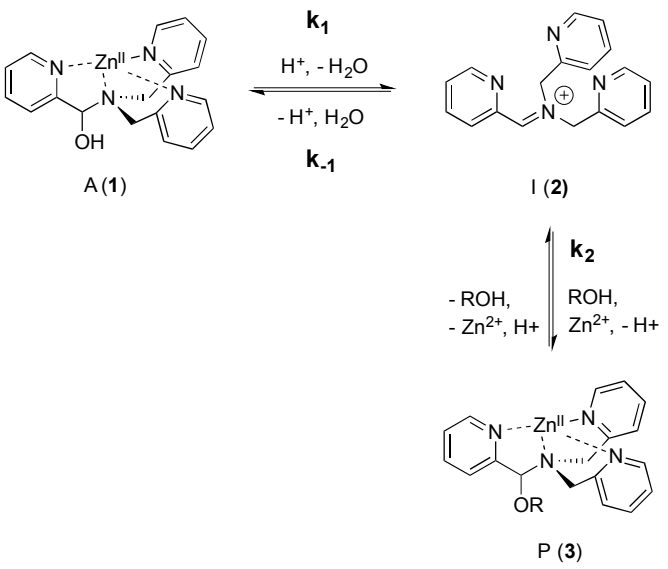

$$\frac{d[P]}{dt} = \frac{k_1 k_2 [A][\mathrm{ROH}]}{k_{-1}[\mathrm{H_2O}] + k_2[\mathrm{ROH}]}$$

Scheme 5. Simplified mechanism and associated rate equation.

This kind of kinetics is referred to as saturation kinetics, and it is indicative of a pre-equilibrium prior to the formation of a high energy intermediate that then reacts with the alcohol. Taking the values of the initial slopes in Figure 3, where the concentration of alcohol was the only variable, leads to the graph shown in Figure 4. Zero order dependence of alcohol in the reaction was verified as a plateau in this plot. The experiments given above, however, do not distinguish as to whether the loss of Zn(II) or the loss of water is the slow step leading to the intermediate.

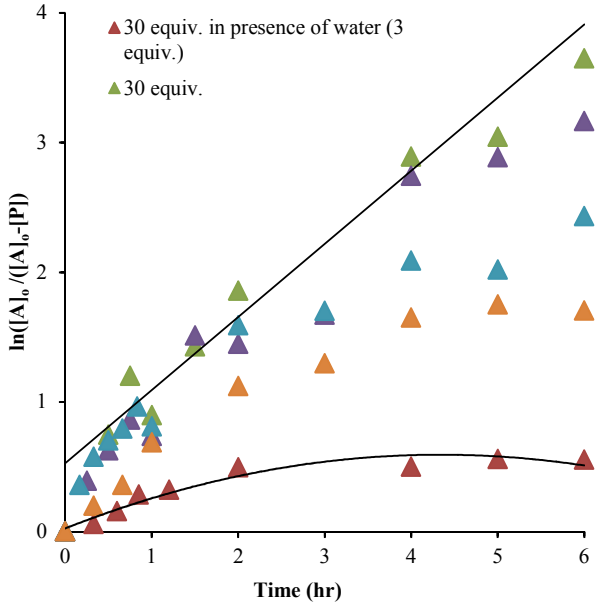

Figure 3. A plot of $\ln([A]_o/([A]_o-[P])$ versus time as a function of the equivalents of alcohol. A is hemi-aminal **1** and P is **3**. (All experiments: 35 mM of 2-PA and Zn(II) was used for the assembly reaction.)

Chemical Science Accepted Manuscript

This journal is © The Royal Society of Chemistry 2014

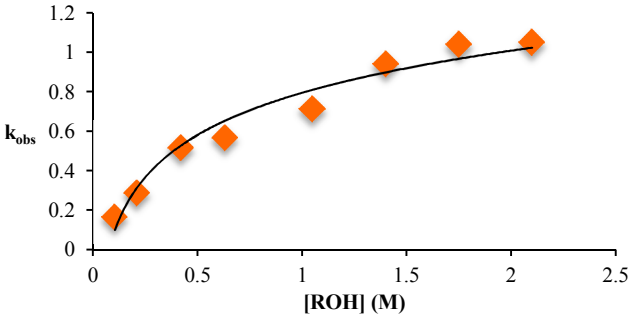

Figure 4. The variation in k_{obs} as a function of the starting concentration of alcohol. Concentration of 2-PA was 35 mM for all experiments.

The mechanism given in Scheme 4 has analogous steps leading to the intermediate, either starting from reactant **1** or product **3**. The difference is the departure of water or departure of alcohol directly before formation of intermediate **2**. The rate of departure of water is predicted to be slower than that of alcohol departure due to the increased stability of the hemi-aminal over the hemi-aminal ether, as revealed from the equilibrium constant measured (see above). However, the difference in the rate of loss of Zn(II) from either the hemi-aminal **1** or the hemi-aminal either **3** is likely minimal. Thus, to reveal whether metal loss or leaving group departure is the slow step in formation of the intermediate(s), we followed the time course for the forward and reverse reaction during the initial period of the transformations. The reactions involve the addition of alcohol to **1** or water to **3**. All experiments were performed with concentration of 2-PA being 0.035 M, and alcohol or water fixed at 0.175 M. By fitting a linear line to the first 10% of reaction, we were able to estimate rate constants of the two reactions. We find rate constants that are approximately the same (0.30 hr^{-1} *vs* 0.35 hr^{-1}). This was the first experiment that indicated that the rate-determining step in hemi-aminal to hemi-aminal ether is loss of the metal.

Although the forward and reverse rate constants are approximately the same, thereby indicating that the rate-determining steps for the forward and reverse reactions are both likely the loss of Zn(II), it is true that the rate from hemi-aminal ether back to hemi-aminal is slightly faster, as would be predicted because an ROH is anticipated to be a better leaving group. Thus, we sought even stronger evidence that the loss of Zn(II) is rate-determining, and therefore we performed a Hammett linear free energy analysis.

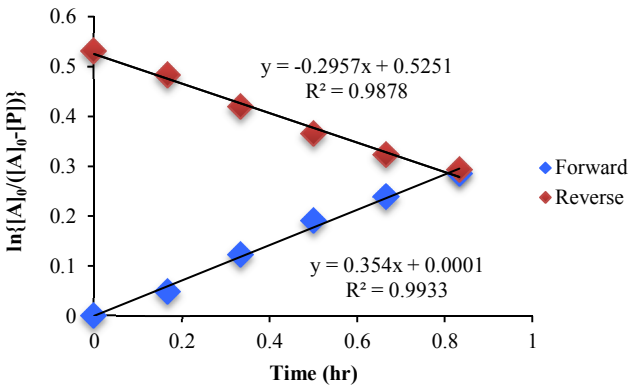

Figure 5. A plot of ln $[A]_o/[A]$ *vs* time in forward and reverse reactions only over the first 10% of reaction.

IV. Hammett Analysis

To further explore the reaction mechanism a Hammett plot was generated. By plotting the $\log(k_X/k_H)$ values for various substituted 2-PA's versus the sigma (σ) electronic substituent constant a Hammett plot was generated. Hammett plots are informative because they show how reaction mechanisms vary as a function of the electronic changes induced by substituents.[38]

A series of 2-pyridinecarboxaldehyde derivatives bearing electron-donating or electron-withdrawing substituents that are para to the aldehyde were investigated for the reaction of **1** to **3** using 4-penten-2-ol as the alcohol (**Figure 6**). From the Hammett plot (log (k_X/k_H) versus sigma[39]), rho was obtained as the slope. Rho describes the sensitivity of the reaction to substituent effects. The calculated rho value from the graph is positive. This leads to the conclusion that negative charge is building during the rds of the assembly, or alternatively there is a loss of positive charge.

The two possible rate-determining steps for the formation of intermediate **2** either involve loss of the Zn(II) cation or formation of a positive iminium, respectively. Loss of a cation is analogous to increased negative charge, whereas formation of an iminium involves creation of a positive charge. Because a positive rho value was found, this supports loss of Zn(II) as the rds in the conversion of **1** to **3**, as was also supported by the fact that the forward and reverse reaction rate constants of Scheme 5 are basically the same.

A Hammett plot using σ^+ was also generated (see supporting information). Such a Hammett plot includes resonance, whereas σ primarily reflects induction. The plot using σ^+ contained significantly more scatter, with a R^2 value of 0.84 compared to the normal Hammett plot (R^2 of 0.977). This is in further accordance with our conclusion that the rds is the loss of Zn(II). If the rds was instead the loss of water, we would predict a better Hammett plot with σ^+ because **2** is stabilized via direct resonance with the substituents. However, the substituents primarily effect metal chelation via induction.

Chemical Science Accepted Manuscript

A)

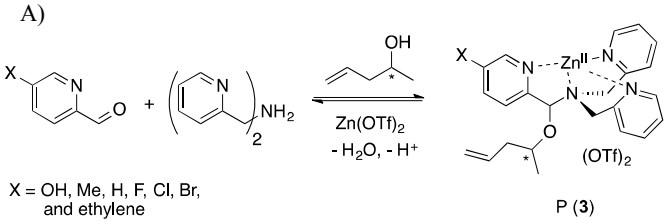

X = OH, Me, H, F, Cl, Br, and ethylene

P (**3**)

B)

X	σ_{para}	log (k_X/k_H)
OH	-0.38	-0.21
Me	-0.14	-0.062
H	0	0
F	0.15	0.15
ethylene	0.23	0.13
Cl	0.24	0.17
Br	0.26	0.16

C)

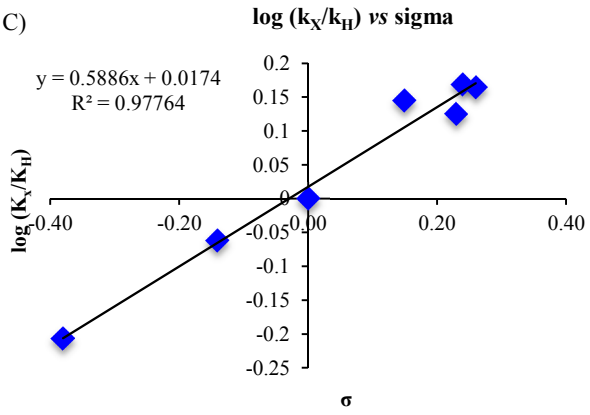

Figure 6. A) Four-component covalent assembly reactions with various R-X structures. B) σ_{para} values[38,39] and corresponding log (k_X/k_H) values for encountered substituents. C) Hammett plot for four-components assembly with para substituted 2-picolinaldehyde.

V. Tying It All Together

The experiments described above allow one to create a qualitative reaction coordinate diagram (**Figure 7**) for the interconversion of **1** (A) and **3** (P). First, because the equilibrium constant for the reaction is less than 1, the energy of A and alcohol is placed lower than P and water (ΔG^o). Second, because the loss of Zn(II) from A and P was found to have the similar rate constants, the barriers leading from A and P to L1 and L2, respectively, are placed the highest on the diagram and their activation energies are comparable ($\Delta G_1^{\ddagger} = \Delta G_2^{\ddagger}$). Next, we place intermediate I in the center of the diagram, which our results support as being **2** rather than **5**. Third, because water is a better nucleophile than an alcohol, the barrier from I to L1 ($\Delta G_{L1}^{\ddagger}$) is drawn lower than the barrier of I to L2 ($\Delta G_{L2}^{\ddagger}$). The remaining question is the relative energies of L1 and L2, and whether their energy difference is similar to the difference in their activation energies to achieve I. However, we postulated above that the bond strengths between OH and OR in A and P likely do not change significantly whether or not Zn(II) is bound. Thus fourth, the energy difference between L1 and L2 should be similar to that between A and P. This reasoning led to the qualitative placement of L1 and L2 on the diagram. The third and fourth insights used here to generate the reaction coordinate diagram also led to the conclusion that the activation energy to create I from L1 is higher than from L2 to I. This is consistent with the notion that an alcohol is a better leaving group than water.

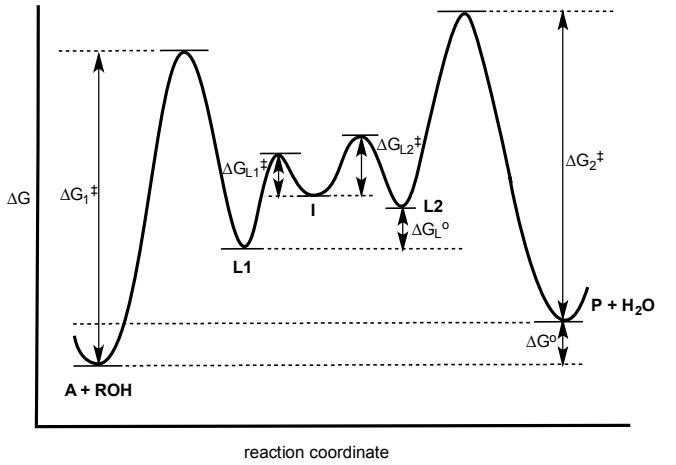

Figure 7. Hypothesized reaction coordinate diagram for multi-component assembly reaction. See Scheme 4 for identity of **A**, **L1**, **L2**, **I** and **P**.

Conclusion

Mechanistic studies of the four-component assembly involving 2-PA, DPA, Zn(II), a secondary alcohol, and catalytic acid revealed several insights. First, the equilibrium lies toward hemi-aminal **1**, and thus the creation of a high yield of **3** requires molecular sieves. Further, the reaction can be driven toward **3** via the use of excess alcohol. Attempts to isolate the previously postulated iminium **2** instead led to the isolation of a pyridinium salt **5**. Yet, **5** does not give the correct products and its formation is not allowed via Baldwin's rules, and thus **5** must form slower than reaction of **2** with water or alcohols. The transformation of **1** to **3** is first order in **1** and zero order in alcohol only at high alcohol concentration, thus showing saturation kinetics in alcohol, analogous to an S_N1 reaction. This supports the creation of a high-energy intermediate that reacts in a fast step with alcohol. The rate-determining step to creation of this intermediate is not the acid-catalyzed expulsion of water, but rather the decomplexation of Zn(II) from the assembly. This conclusion is supported both by the fact that the forward and reverse rate constants for interconversion of **1** and **3** are basically the same, and by a positive Hammett rho value that supports loss of positive charge in the rds. The mechanistic insights given herein should be informative for other dynamic reactions involving interconversions of hemi-aminals to hemi-aminal ethers.

Acknowledgements

Chemical Science Accepted Manuscript

This journal is © The Royal Society of Chemistry 2014

EA gratefully acknowledges the financial support from the National Institutes of Health (R01GM077437), the Welch Foundation (F-1151), and the National Science Foundation (CHE-1212971). KD thanks the support by NIH (GM059802), and the Welch Foundation (F-1390).

Notes and references

1. Y. Jin, C. Yu, R. J. Denman, and W. Zhang, *Chem. Soc. Rev.*, 2013, **42**, 6634-6654.
2. G. Gasparini, M. Dal Molin, A. Lovato and L. J. Prins, in *Supramolecular Chemistry*: *From Molecules to Nanomaterials*, ed. J. W. Steed and P. A. Gale, John Wiley & Sons, Ltd, 2012, DOI: 10.1002/9780470661345.
3. B. L. Miller, *Dynamic Combinatorial Chemistry*, John Wiley & Sons, 2009.
4. P. T. Corbett, J. Leclaire, L. Vial, K. R. West, J.-L. Wietor, J. K. M. Sanders, and S. Otto, *Chem. Rev.*, 2006, **106**, 3652–3711.
5. J.-M. Lehn, *Chem. Soc. Rev.*, 2007, **36**, 151–160.
6. R. J. Wojtecki, M. A. Meador, and S. J. Rowan, *Nat. Mater.*, 2011, **10**, 14–27.
7. A. Wilson, G. Gasparini, and S. Matile, *Chem. Soc. Rev.*, 2014, **43**, 1948–1962.
8. X. Jiang, Y.-K. Lim, B. J. Zhang, E. A. Opsitnick, M.-H. Baik, and D. Lee, *J. Am. Chem. Soc.*, 2008, **130**, 16812–16822.
9. Y. Yang, X.-L. Pei, and Q.-M. Wang, *J. Am. Chem. Soc.*, 2013, **135**, 16184–16191.
10. P. Vongvilai and O. Ramström, *J. Am. Chem. Soc.*, 2009, **131**, 14419–14425.
11. S. J. Rowan, S. J. Cantrill, G. R. L. Cousins, J. K. M. Sanders, and J. F. Stoddart, *Angew. Chem. Int. Ed. Engl.*, 2002, **41**, 898–952.
12. A. Herrmann, *Chem. Soc. Rev.*, 2014, **43**, 1899–1933.
13. J.-M. Lehn, *Top. Curr. Chem.*, 2012, **322**, 1–32.
14. S. P. Black, J. K. M. Sanders, and A. R. Stefankiewicz, *Chem. Soc. Rev.*, 2014, **43**, 1861–1872.
15. Y. Jin, Q. Wang, P. Taynton, and W. Zhang, *Acc. Chem. Res.*, 2014, **47**, 1575–1586.
16. F. F. Aricó, T. T. Chang, S. J. S. Cantrill, S. I. S. Khan, and J. F. J. Stoddart, *Chem. Eur. J.*, 2005, **11**, 4655–4666.
17. P. Hadik, L.-P. Szabó, and E. Nagy, *Desalination*, 2002, **148**, 193–198.
18. M. T. Reetz, T. Sell, A. Meiswinkel, and G. MehlerK, *Angew. Chem. Int. Ed.,* 2003, **42**, 790-793.
19. R. Eelkema, R. A. van Delden, and B. L. Feringa, *Angew. Chem. Int. Ed.,* 2004, **43**, 5013-5016.
20. J. Long, J. Hu, X. Shen, B. Ji, and K. Ding, *J. Am. Chem. Soc.*, 2002, **124**, 10-11.
21. L. You, J. S. Berman, and E. V. Anslyn, *Nature. Chem.*, 2011, **3**, 943–948.
22. L. You, S. R. Long, V. M. Lynch, and E. V. Anslyn, *Chem. Eur. J.*, 2011, **17**, 11017–11023.
23. L. You, G. Pescitelli, E. V. Anslyn, and L. Di Bari, *J. Am. Chem. Soc.*, 2012, **134**, 7117–7125.
24. L. You, J. S. Berman, A. Lucksanawichien, and E. V. Anslyn, *J. Am. Chem. Soc.*, 2012, **134**, 7126–7134.
25. G. Li, F. R. Fronczek, and J. C. Antilla, *J. Am. Chem. Soc.*, 2008, **130**, 12216–12217.
26. A. Star, I. Goldberg, and B. Fuchs, *Angew. Chem. Int. Ed. Engl.*, 2000, **39**, 2685–2689.
27. B. Fuchs, A. Nelson, A. Star, J. F. Stoddart, and S. Vidal, *Angew. Chem. Int. Ed. Engl.*, 2003, **42**, 4220–4224.
28. J. P. Mason and H. W. Block, *J. Am. Chem. Soc.*, 1940, **62**, 1443.
29. S. Lakhdar, T. Tokuyasu, and H. Mayr, *Angew. Chem. Int. Ed. Engl.*, 2008, **47**, 8723–8726.
30. J. E. Baldwin, *J. Chem. Soc., Chem. Commun.* 1976, 734-736
31. J. E. Baldwin, R. C. Thomas, L.I. Kruse, L. Silberman, *J. Org. Chem.*, 1977, **42**, 3846–3852
32. S. Eldin, and W. P. Jencks, *J. Am. Chem. Soc.*, 1995, **117**, 4851–4857.
33. S. Eldin, J. A. Digits, S-T. Huang, and W. P. Jencks, *J. Am. Chem. Soc.*, 1995, **117**, 6631–6632.
34. S. Eldin, and W. P. Jencks, *J. Am. Chem. Soc.*, 1995, **117**, 9415–9418.
35. K. N. Dalby, and W. P. Jencks, *J. Am. Chem. Soc.*, 1997, **119**, 7271–7280.
36. R. G. Pearson, H. R. Sobel, and J. Songstad, *J. Am. Chem. Soc.*, 1968, **90**, 319–326.
37. J. Mendham, R. C. Denney, J. D. Barnes, and M. J. K. Thomas, *Vogel's Quantitative Chemical Analysis (6th Edition)*, Prentice Hall, 6th ed. 2000.
38. C. D. Ritchie and W. F. Sager, *Prog. Phys. Org. Chem.*, 1964, **2**, 323-400.
39. R. Chen, K.-C. Zhang, L. Liu, X.-S. Li, and Q.-X. Guo, *Chem. Phy. Lett.*, 2001, **338**, 61–66.

Chemical Science Accepted Manuscript